

Design of a Novel Biaxial Loading Fixture Integrated Into Uniaxial Testing Machines



Brilliant Gustavo Purnawan

Andhika Djajadi

Yuriy Kim

Magzhan Koshkarov

Sam Koplickat

Table of Contents

1	Selection & evaluation process	2
1.1	Selection Matrix Table	
1.2	Justification of evaluation process	
2	Comprehensive overview of final design	5
2.1	Overview of Final Design	
2.2	Detailed View of Final Design	
2.3	Fixture Measurement sensors	
2.4	Grippers	
2.5	Testing Rig different Loading Ratio Configuration	
3	Explanation of Design	10
4	Alignment with Sustainable Development Goals (SDGs)	14
5	References	16

1 Selection & evaluation process

1.1 Selection matrix Table

1	Weighting	Design 1 (Brilliant)		Design 2 (Andhika)		Design 3 (Yuriy)		Design 4 (Magzhan)		Design 5 (Sam)	
		PF	Score	PF	Score	PF	Score	PF	Score	PF	Score
1. Ability of the device to fit to the Zwick/Roell Z250 SN/SW (Type 2) testing machine without requiring any modifications to the testing machine.	3	5	15	2	6	2	6	1	3	2	6
2. Ability of the device to test the specified cruciform specimens.	3	4	12	4	12	4	12	4	12	4	12
3. Ability of the device to perform tension-tension, compression-compression, and tension-compression tests under the following loading ratios: ± 0.5 and ± 1 . The loads must be provided by the testing machine only (extra actuators are not allowed).	3	4	12	4	12	4	12	4	12	4	12
4. Ability of the fixture to measure the applied loads along each axis (maximum applied load in each axis: 100kN) as well as the deformation of the specimen (maximum displacement in each axis: 10mm). (Inclusion of load cell to measure load or extensometer to measure deformation)	3	2	6	2	6	2	6	3	9	2	6
5. Alignment ability of the fixture for not creating any bending moments or shear forces on the specimen being tested.	3	4	12	3	9	3	9	4	12	3	9
6. Ability of the fixture for keeping the centre of the test specimen in its original position during the testing.	2	5	10	4	8	4	8	4	8	4	8
7. The design of the specimen clamps must be compatible with the testing machine.	3	4	12	4	12	1	3	4	12	2	6
8. A maximum of two people (skilled and trained mechanical/electrical engineer) must be able to set-up the fixture.	2	4	8	2	4	2	4	1	2	2	4
9. Maximum time for the reconfiguration of the device must be less than 30 minutes.	1	5	5	3	3	4	4	3	3	3	3
10. The device must not require servicing more than once every six months.	2	4	8	4	8	4	8	3	6	4	8
11. The fixture must comply with selected relevant health and safety regulations.	3	3	9	3	9	3	9	4	12	3	9
12. The design of the fixture must exhibit some degree of compliance with appropriate Ecodesign principles.	2	3	6	3	6	4	8	4	8	3	6
Total score		115		95		89		99		89	

Weighting Factor	
Low Importance	1
Medium Importance	2
High Importance	3

Performance Factor	
Unsuitable	0
Just Suitable	1
Adequate	2
Quite Suitable	3
Good	4
Very Suitable	5

Table 1: Selection Matrix Table with weighting factor and performance factor

1.2 Justification of evaluation process

As seen in *Table 1* the performance factor method using weight factors was used to evaluate the most suitable design. The scores per solution are summed up in the performance factor method, and the highest solution is the optimal solution. As seen in *Table 1*, the performance factor ranges from 0-5, where 5 signifies very suitable. However, this scoring scheme assumes that all requirements are equally important, which is not the case. Hence, each factor is assigned a weighting factor, highlighting its importance. The total score is found using the formula:

$$\sum_{i=1}^{12} WFi \cdot PFi$$

As seen on *Table 1*, the weight factor ranges from 1 - 3, with 3 being the most important. Considering this design project, there are 7 crucial design criteria, particularly specifications 2 and 3, as the entire device practicality lies around the premise of testing a cruciform specimen with the ability to perform tension-tension, compression-compression, and tension-compression tests under the following loading ratios: ± 0.5 and ± 1 . However, for example, specification 9 was assigned the lowest weight factor of 1 comparatively, as taking more time to reconfigure the device would not negatively affect it. Specification 8 was given a weight factor of 2, since requiring more than 2 engineers to set up the device will not affect it; however, it would increase costs. As seen in Table 1, design 1 has the highest total score of 115, whereas the other designs have lower scores. Even though all the designs have a score of 4 in specifications 2 and 3, as that is essentially the premise of the design project, it is in specifications 1 and 7, where, for example, design 1 shows a much-improved score (5) and (4) respectively compared to for example design 5 who has a score of 1 and 2 respectively. This is because, as seen in Task 2 below, design 1 properly integrates with type 2 of the Zwick/Roell Z250 SN/SW without needing any adjustments, and its clamps are correctly compatible.

In contrast, for design 5 it needs to integrate better with type 2, due to a load only applied from the top, and moreover, the clamps used are bulky. Furthermore, it can be noticed that designs 3 and 5 have the same score of 89, with different scores in the respective specifications since their designs had similarities in some aspects of their

concepts. It can be seen that design 1, has a score of 2 for specification 4, because load cells and extensometers were not added; however, this can be implemented to improve the design.

2 Comprehensive overview of final design

2.1 Overview of Final Design

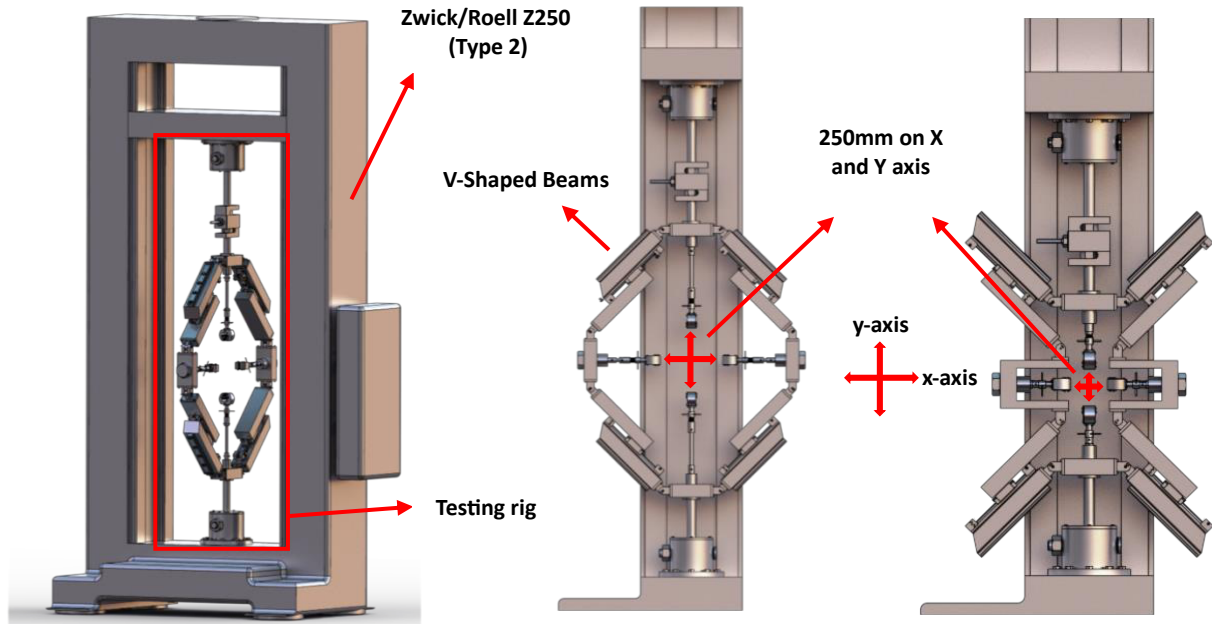


Figure 1: isometric view of biaxial testing machine

Figure 2: Side view of biaxial testing rig.

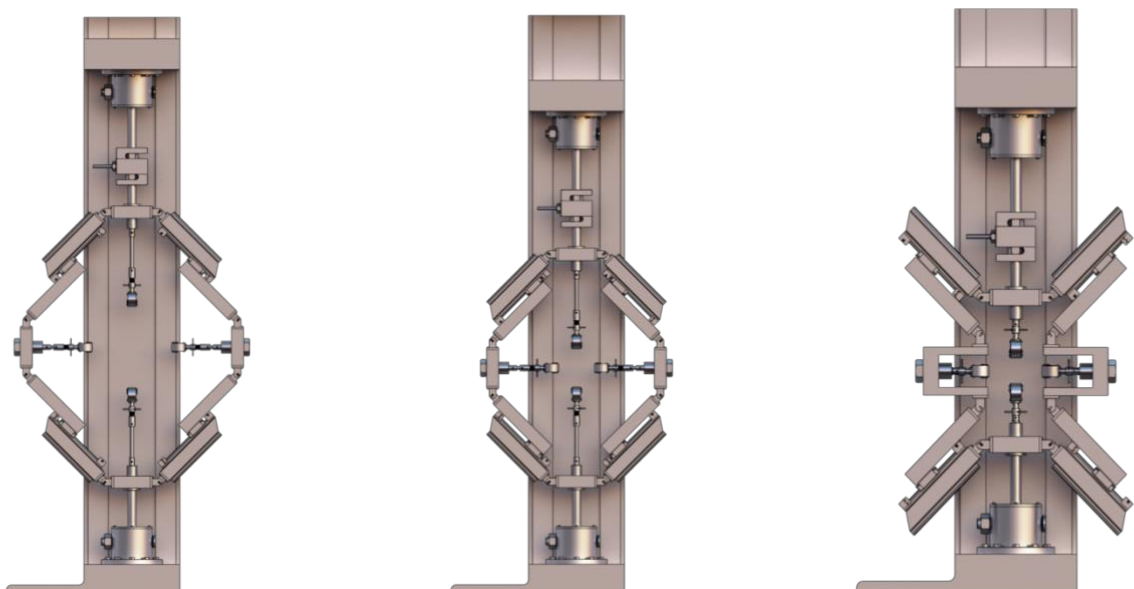


Figure 3: Tension-tension testing.

Figure 4: Compression-compression testing.

Figure 5: Compression-tension testing.

2.2 Detailed View of Final Design



Figure 6: Vertical axis V-bracket.

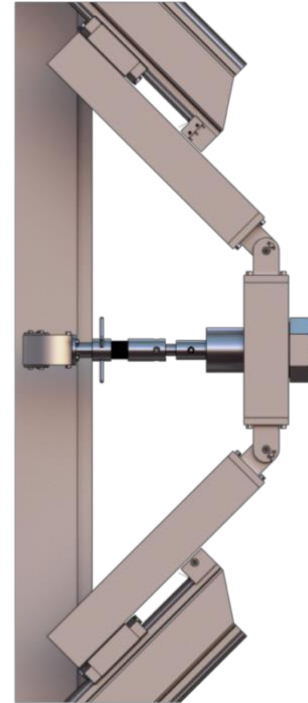


Figure 7: Horizontal axis V-bracket.

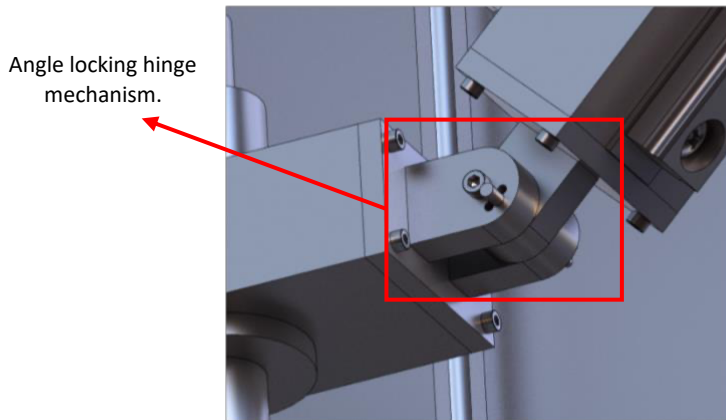


Figure 8: Rib reinforced L-bracket hinge.

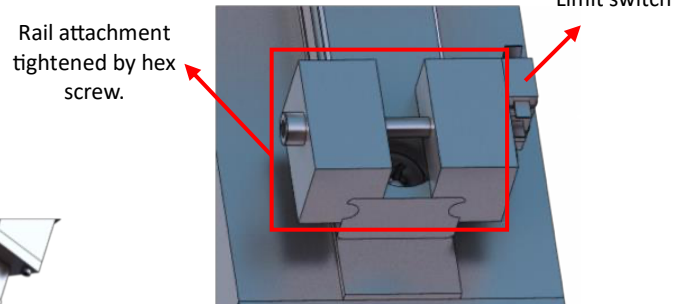


Figure 9: Limit switch and rail attachment.

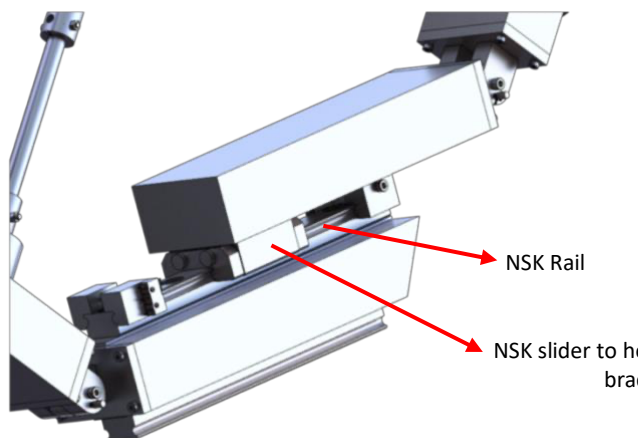


Figure 10: Extension arm connection, NSK rails and slider



Figure 11: Bottom fixture to Zwick/Roell machine adaptor



Figure 12: Top fixture to Zwick/Roell machine adaptor

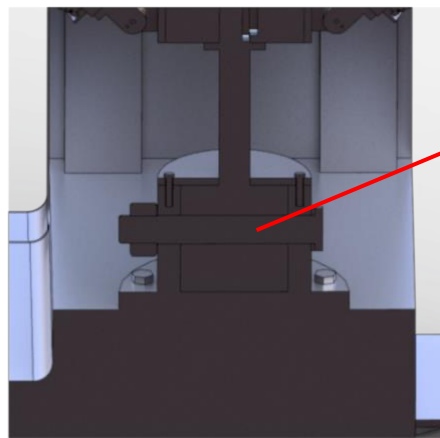


Figure 13: Section view of fixture to Zwick/Roell machine adaptor

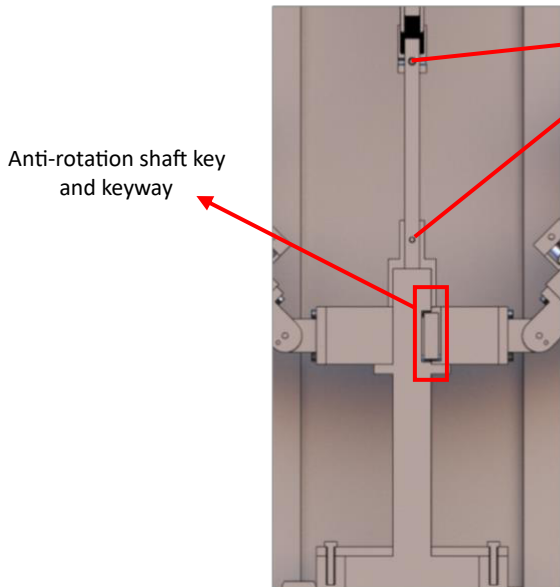


Figure 14: Section view of V-bracket base rod adaptor to grippers

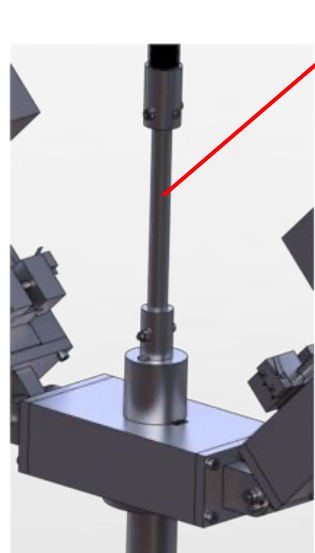
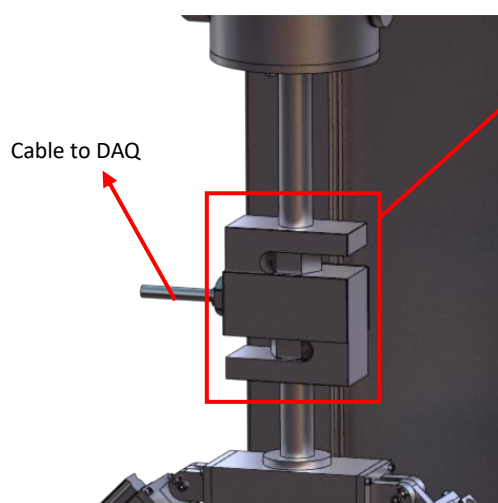


Figure 15: V-bracket base rod adaptor to grippers

2.3 Fixture Measurement sensors



Forsentek 100kN S-type tension/compression load cell

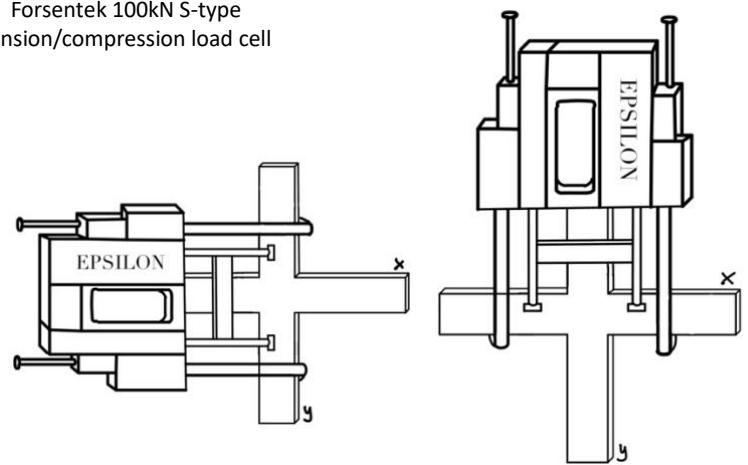


Figure 16: Load cell suspended between fixture and Zwick/Roell adaptor.

Figure 17: Dual epsilon extensometer setup on both specimen axis.

2.4 Grippers

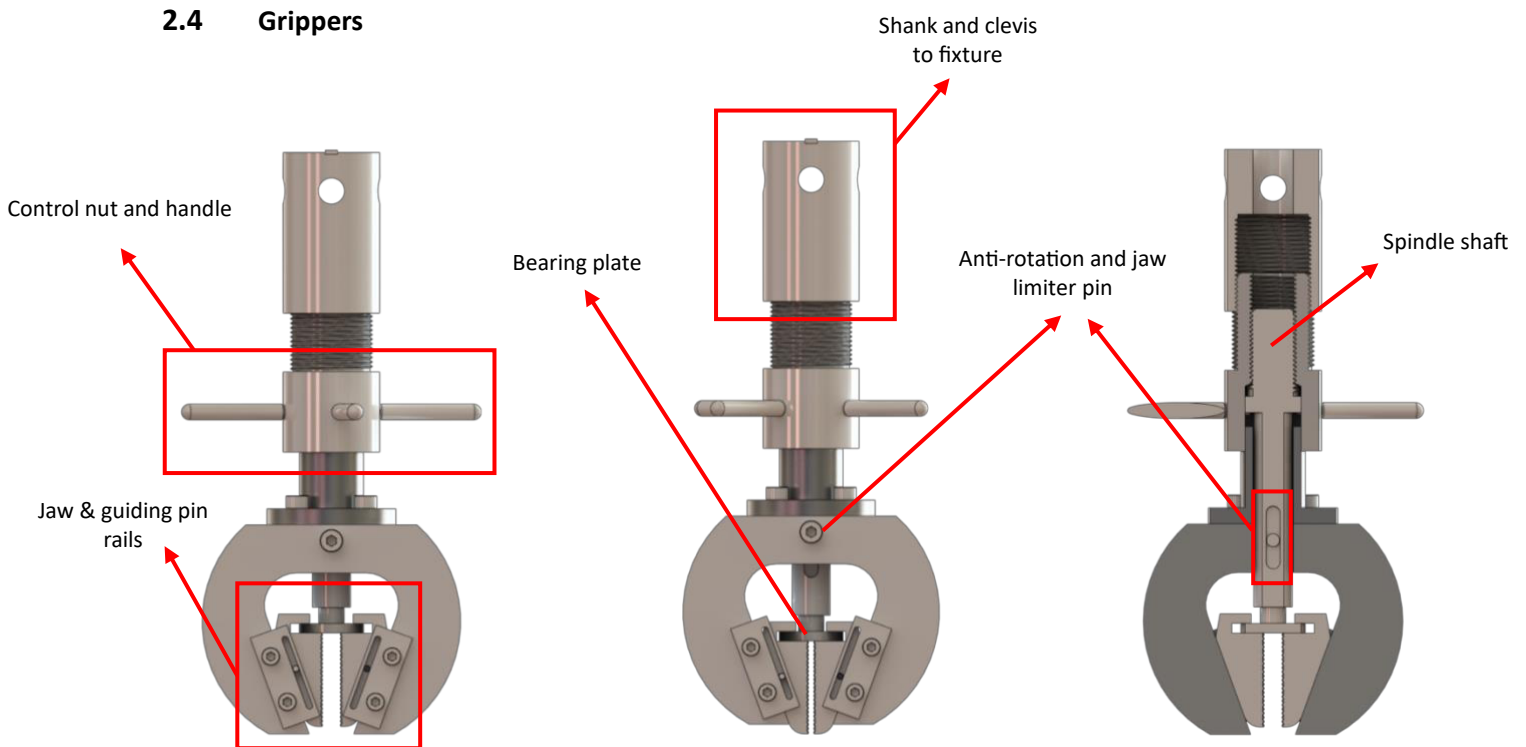


Figure 18: Wedge action tensile grippers open jaw.

Figure 19: Wedge action tensile grippers closed jaw.

Figure 20: Section view of wedge action tensile grippers.

2.5 Testing Rig different Loading Ratio Configuration

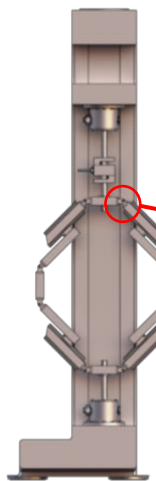


Figure 21: Compression-compression/Tension-tension 1:1 loading ratio.

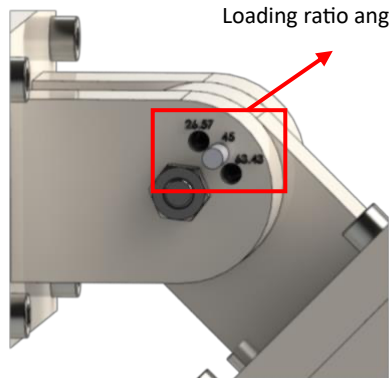


Figure 22: 45-degree joint angle.

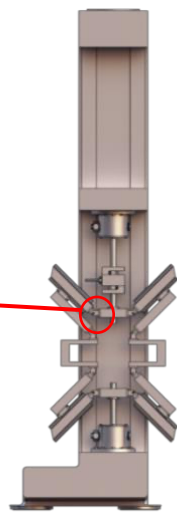


Figure 23: Compression-tension 1:1 loading ratio.

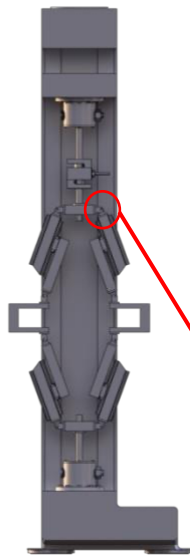


Figure 24: Compression-compression/Tension-tension 1:0.5 loading ratio.

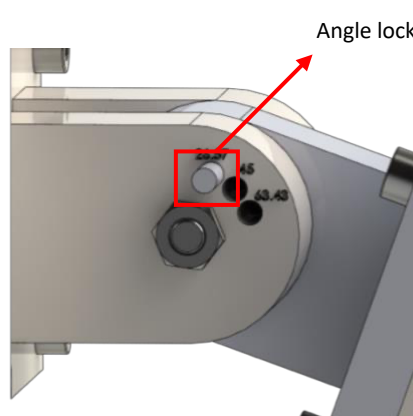


Figure 25: 26.57-degree joint angle.

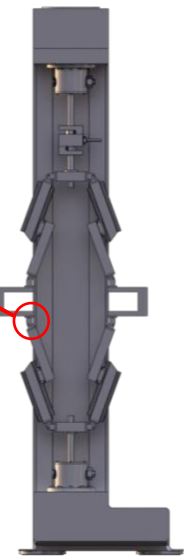


Figure 26: Tension-tension 1:0.5 loading ratio extended.

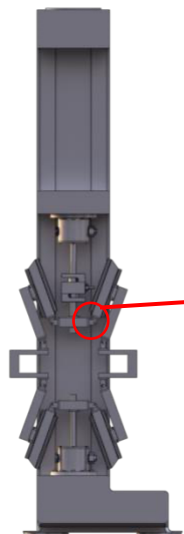


Figure 27: Compression-tension 1:0.5 loading ratio.

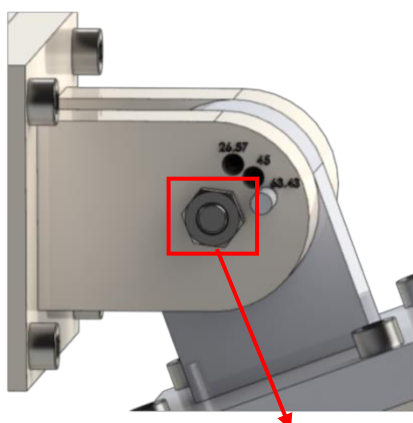


Figure 28: 63.43-degree joint angle.



Figure 29: Compression-tension 1:0.5 loading ratio extended.

3 Explanation of Design

The operation of the final design fixture is done through the suspension of 4 V-shaped beam structures, 2 beams parallel and facing each other in the x-axis and 2 beams parallel and facing each other in the y-axis. These V-shaped beam structures are supported by a rod on each of the y-axis beams, connected to an adaptor for the Zwick/Roell Z250 (Type 2) machine, shown in *Figure 1*.

The final design features a fixture integrating four V-shaped beams arranged in opposing pairs along the x and y axes. Each y-axis beam is bolstered by a support rod and seamlessly interfaces with the Zwick/Roell Z250 machine through custom-engineered adapters. Rails and sliders ensure the interconnection between the x and y-axis beams, ensuring smooth load transfer application across the biaxial setup and maintaining specimen integrity, with one V-shaped beam on one axis connected to two V-shaped beams on the perpendicular axis at its end. This fixture enables precise and configurable setups for compression-compression, tension-tension, and compression-tension testings. A visual setup shown in *Figure 1*, detailing the fixture's default compression-compression/tension-tension at a 1:1 loading ratio layout.

This fixture design allows compression-compression, tension-tension, and compression-tension testings by the V-shaped beam orientations. The adjustable gripper gaps are set by default at 250 mm in its initial position when no tension or compression is applied to the specimen. This neutral position is achieved when the sliders are positioned centrally on the rails; details in *Figure 2*. While the testing can exceed the maximum displacement requirements of 10 mm, a limit switch is integrated into the rails, thus restricting movement tailoring to various test requirements.

For tension-tension testing, due to the interconnectivity of the V-shaped beams through the rails in both axes, as the Zwick/Roell machine rises in the y-axis, the x-axis beams will also move backward, thus tensioning the specimen on both axes; this setup is seen in *Figure 3*. Similarly, for compression-compression testing, as the Zwick/Roell machine compresses in the y-axis, the x-axis beams will move inwards, compressing the specimen on

both axes; setup in *Figure 4*. However, in compression-tension testing, the V-shaped beams must be inverted. Thus, as the Zwick/Roell machine rises in the y-axis, tensioning the specimen, it will move the x-axis inwards, compressing the specimen. This is also applicable vice versa. Visuals on this are depicted in *Figure 5*. However, an extension on its central beam of the V-shaped beams on the x-axis is shown to accommodate the gripper length.

Elaborating on the V-shaped beam design, it consists of a central beam and two extension beams positioned at a specific example. Each y-axis V-shaped beam is connected to two x-axis V-shaped beams on each of the y-axis extension beams through rails and sliders, as shown in *Figure 6*. Similarly, one x-axis V-shaped beam is connected to two y-axis V-shaped beams on its extension beams, *Figure 7*. This interconnectivity between 4 beams forms a diamond structure, creating a link of load transfer across its rails. The central beam is connected to the extension beam through a rib reinforced hinge mechanism, with an angle locking pin to prevent beam rotation, as shown in *Figure 8*. On the y-axis extension beams, there is a bolted NSK rail with limit switches on either end to prevent overextension. The rails are attached on both ends to accommodate modular testing configurations. To complete the movement, NSK sliders are attached to the x-axis extension beams. The slider and rail configuration on the extension beam are shown in *Figure 10*. The limit switch is attached to a rail rig attachment, gripping the rails via a hex screw, thus enabling the adjustment of the limit switch position, seen in *Figure 9*.

The central beams on the y-axis feature a rod that will suspend the fixture, connected by a custom adaptor to the Zwick/Roell machine secured by a clevis pin to prevent rotation. This setup is seen in *Figures 11 - 13*. The central beam and gripper are connected through a shaft key and keyway mechanism on the inner part of the central beam and the rod adapter. This also prevents unwanted torsion on the specimen due to the grippers. Clevis pins are ideally applied on the adaptors and the gripper to prevent further rotation of the rods, as shown in *Figures 14 & 15*.

A Forsentek load cell is integrated between the upper machine adaptor and the y-axis central beam to measure the applied load, depicted in *Figure 16*. A dual epsilon extensometer is integrated into each specimen axis to measure displacement, as shown in

Figure 17. The grippers are tightened and loosened by rotating the control nut, which will either move the spindle shaft downwards or upwards. The bearing plate of the spindle shaft is connected to the jaws, which are stabilized by the guiding pin rails ensuring smooth closing and opening of the jaws, *Figures 18 & 19*. A keyway and limiter pin are added on the spindle shaft shown in *Figure 20* to prevent over-rotation and extension.

To allow various loading ratios of ± 0.5 and ± 1 . The hinge mechanism between the central and extension beams features multiple-angle pin holes, indicated by the engraved angle positions. For 1:1 loading ratio of all testing configurations, all hinges are set at 45° , *Figures 21 - 23*. For the 1:0.5 loading ratio of compression-compression and tension-tension, the y-axis hinges are set at 63.43° , and the x-axis hinges at 26.57° , *Figures 24 - 26*. Lastly, the V-shaped beams are inverted for a 1:0.5 loading ratio of compression-tension, setting the y-axis hinges to 63.43° , and the x-axis hinges to 26.57° , *Figures 27 - 29*.

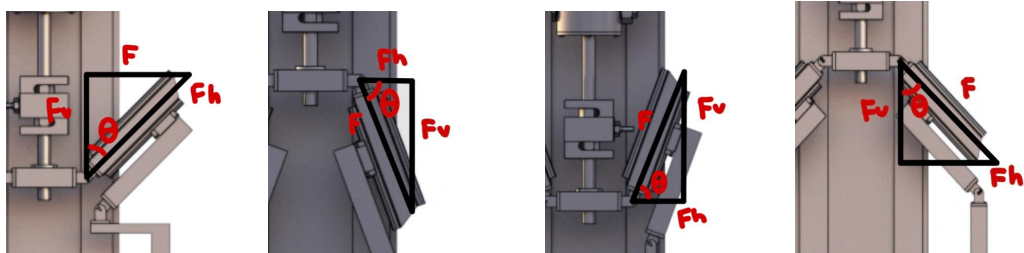


Figure 30: Horizontal forces, vertical forces and incidence angle geometrical analysis

This angle configuration is chosen through geometrical analysis. The fixture system is symmetric about the central axis. A load ratio is the proportionality between vertical and horizontal forces applied to the specimen. Thus, defining the vertical (F_v) and horizontal (F_h) force components in relation to the applied force, we calculated the angle of incidence. For load ratio 1, resultant forces in horizontal and vertical planes must be equal, thus,

$$\sin(\theta) = \cos(\theta)$$

Through the unit circle, this equality is found at 45° . Hence, for a load ratio of 1:1 all eight joints need to be adjusted to a 45° angle. For a load ratio of 0.5, the horizontal force is defined to be half the magnitude of the vertical force.

$$\frac{F_v}{F_h} = 2$$

$$\frac{F \times \sin(\theta)}{F \times \cos(\theta)} = 2$$

$$\tan(\theta) = 2$$

By resolving θ , four hinges are set at an angle of 63.43° and the other four 26.57° .

4 Alignment with Sustainable Development Goals (SDGs)

Our material testing machine final design could represent a change in testing technology, particularly in SDG 9: Industry, Innovation, and Infrastructure. This cutting-edge machine offers high-precision and versatile testing capabilities across various materials, providing a platform for accelerated experimentation and innovation in developing resilient and sustainable infrastructure. Researchers can efficiently simulate real-world conditions with advanced control systems and automation features. For instance, our design can be utilized to evaluate bio-based construction materials, ensuring they meet rigorous standards for strength, durability, and environmental impact. This opens possibilities for creating innovative, durable, and eco-friendly materials and equips researchers to address the growing demands for sustainable infrastructure.

Beyond SDG 9, our design can be addressed in SDG 12: Responsible Consumption and Production. Precision in understanding load-bearing limits, as seen in testing steel alloys, can prevent over-engineering, ensuring structures are robust without unnecessary material excess. This precision-driven approach optimizes resource use, allowing efficient and economical designs to be selected, ultimately minimizing waste in construction projects. For example, our design can be applied to test new alloys for sustainable construction, guaranteeing the required strength while minimizing environmental impact. This aligns with responsible consumption and production principles by efficiently utilizing resources and reducing environmental impact. Our design further contributes to SDG 12 by enforcing sustainability criteria in production. Testing material durability and life cycle ensure that only materials meeting high sustainability standards are considered, reducing waste. For instance, our design can assess the durability of materials in electronic devices, ensuring adherence to high sustainability standards. Proactively minimizing premature failures reduces the need for replacements and mitigates waste, offering the potential for a more sustainable production process. Our design's selective use of materials can withstand extended use and align with eco-friendly practices, minimizing the environmental impact of material disposal and replacement.

Addressing SDG 13: Climate Action, our design can be instrumental in advancing renewable energy technologies. It can precisely evaluate the mechanical properties of materials used in solar panels and wind turbines, ensuring durability, reliability, and efficiency under challenging environmental conditions. For example, our design can be employed to test new alloys intended for use in solar panels, guaranteeing their efficiency in capturing and converting solar energy. Additionally, our design facilitates the assessment of materials designed to capture, store, or mitigate greenhouse gas emissions. Researchers can use it to test the efficiency of materials used in carbon capture technologies, potentially contributing significantly to the development and optimization of sustainable materials and supporting the transition to cleaner energy sources.

Design can contribute to SDG 13 by testing materials to enhance infrastructure resilience against climate change-related stresses. It enables precise evaluation of the material's performance under various environmental conditions, simulating temperature fluctuations, humidity, and mechanical stresses. Subjecting materials to these conditions can help researchers understand how they respond to climate-induced stresses, offering insights crucial for developing materials that can withstand the challenges posed by climate change. Whether testing for heat resistance, corrosion resistance, or structural integrity, our design can play an essential role in ensuring that materials meet the requirements to enhance infrastructure resilience in the face of evolving climate conditions.

Our material testing machine design exemplifies a multifaceted contribution to sustainable development, aligning with SDGs 9, 12, and 13. Precision testing and innovation serve as versatile tools for advancing technology, promoting responsible consumption and production, and addressing the challenges of climate change.

5 References

- Keil, G. (2022). "M12 Threaded S-Type Tension Compression Load Cell 1000kg". Available at:
<https://grabcad.com/library/m12-threaded-s-type-tension-compression-load-cell-1000kg-1>
- Raja, J. (2021). "Wedge Action Tensile Stress". Available at:
<https://grabcad.com/library/wedge-action-tensile-grips-1>
- Sophiahightech. (2023). "Biaxial Test Fixture". Available at:
<https://www.sophiahightech.com/en/biaxial-test-fixture/>